Correlation of Molecular Organization and Substrate Wettability in the Self-Assembly of n-Alkylsiloxane Monolayers

ARTICLE *in* THE JOURNAL OF PHYSICAL CHEMISTRY · JUNE 1995

Impact Factor: 2.78 · DOI: 10.1021/j100024a049

Correlation of Molecular Organization and Substrate Wettability in the Self-Assembly of *n*-Alkylsiloxane Monolayers

Atul N. Parikh,[†] Bo Liedberg,[§] Sundar V. Atre,[†] Moses Ho,[†] and David L. Allara*[,†,‡]

Departments of Materials Science & Engineering and Chemistry, Pennsylvania State University, University Park, Pennsylvania 16802

Received: February 7, 1995[⊗]

Monolayers of *n*-octadecylsiloxane ($CH_3(CH_2)_{17}SiO_xH_y$; ODS) were self-assembled from *n*-octadecyltrichlorosilane solutions onto a series of OH- and CH_3-containing surfaces prepared from the self-assembly of controlled composition mixtures of $HO(CH_2)_{16}SH$ and $H_3C(CH_2)_{15}SH$ on gold (RS/Au). Using null ellipsometry, infrared spectroscopy, and hexadecane contact angles; the coverages, chain structures, and surface wetting of the formed ODS assemblies were determined as a function of the OH fraction, $f_{OH} \equiv [OH]/[CH_3 + OH]$, in the starting RS assembly. Three distinct ODS adsorption regimes were observed: (1) on pure CH_3 surfaces no stable adsorbed layer forms; (2) for $0.1 \lesssim f_{OH} \lesssim 0.8$, the coverage is incomplete and monotonically increases with f_{OH} and the ODS structures consist of a range of coexisting domains of nearly all-*trans* chains and disordered, liquid-like components with maximum disorder content, estimated as >80%, arising near $f_{OH} \sim 0.5$; and (3) for $f_{OH} > 0.8$, a high coverage, close-packed monolayer is formed with predominantly all-*trans* chains tilted at 8−12° from the surface normal, a distinctly different tilt than the known value of 26−30° for the RS underlayer and an indication of strong structural decoupling (incommensurability) between the two highly organized layers. The f_{OH}-dependence of the structures is explained on the basis of a previously proposed hypothesis that a continuous preadsorbed, substrate-bound water film is required for achieving maximum organization during *n*-alkylsiloxane self-assembly and that, in the present case of the OH/CH_3 surfaces, the required water film structure at the preparation solution/substrate interface is not reached until high f_{OH} values.

1. Introduction

Interest in the preparation of highly organized surface-bound molecular assemblies with molecular level control over the structural order and composition has grown considerably in recent years.[1,2] The development of self-assembled monolayers (SAMs) has received particular attention, and well-known examples of ordered alkyl chain SAMs now exist[2,3] in which the chains appear to approach the ideal rigid-rod limit of all-*trans* conformations with a uniform tilt angle.[4] However, in practice, because of a variety of factors defects will always be present, even for maximum coverage films on atomically flat substrates. Further, at diminished coverages, a large number of partially disordered structural phases will arise, ranging from homogeneous films of uniform density at the molecular scale[5,6] to heterogeneous films of macroscopic patches of organized adsorbate. The exact character of all of the above structures can strongly influence surface properties, such as wetting by liquids,[7,8] and matrix properties, such as charge transport in electrochemical systems.[9] The rational control of film structure depends critically upon a detailed understanding of the self-assembly mechanisms, and two limiting types can be considered: (1) monolayers formed by direct adsorbate bonding to specific substrate lattice site with formation of a superlattice, approximated by alkanethiolates on Au(111)[3,10,11] and (2) monolayers formed with adsorbate organization independent of the substrate structure. Recently, it has been shown that the second case can be approximated by *n*-alkylsiloxane monolayers[2,12] when prepared under conditions of well-hydrated surfaces,[13] particularly on Au,[14,15] where no covalent attachment to the substrate surface is possible. An understanding of the formation mechanism of alkylsiloxane monolayers is important because of the popularity of these films for both scientific and technological applications[2,16] requiring highly dense, hydrophobic and oleophobic coatings. This popularity arises to a great extent because the films can be prepared on many different types of substrates, particularly oxides such as SiO_2, under general preparation conditions involving *n*-alkyltrichlorosilanes in hydrocarbon solutions. This generalized behavior recently has been explained by a proposed substrate decoupling mechanism[13] involving transient *n*-alkylsilanol species which self-assemble upon a continuous ultrathin layer of physisorbed water to form condensed-phase structures, analogous to Langmuir monolayers, whose structures are independent of the substrate surface structure with the organization driven nearly exclusively by intermolecular interactions. A very important aspect of this mechanism is that it implies two distinct classes of structures: (1) uniform, arising for monolayers formed on a continuously wetted substrate, and (2) heterogeneous, arising on incomplete wetted substrates with the structures dependent on the exact distribution of surface water. In the latter case, the structures are unique to this decoupling mechanism and thus may not be accessible by assembly of superlattice types of films. The details of such heterogeneous structures have not been reported, and their characterization would be both an important confirmation of the substrate decoupling mechanism and an indication of new classes of monolayer film structures of potential practical applications requiring controlled defect coatings. One approach to preparing such structures is through the use of a systematic set of precisely controlled water wettability surfaces. Ulman

* Author to whom correspondence should be addressed (e-Mail: dla3@psu.edu).
† Department of Materials Science & Engineering.
‡ Department of Chemistry.
§ While on leave from the Laboratory of Applied Physics, Linköping University, S-581 83, Linköping, Sweden.
⊗ Abstract published in *Advance ACS Abstracts*, June 1, 1995.

0022-3654/95/2099-9996$09.00/0

and co-workers[17] have shown that mixed composition monolayers of OH- and CH_3-terminated *n*-alkanethiolate SAMs on Au (RS/Au) form such a set, and a recent report[18] has shown a correlation between the monolayer composition and the transfer ratio of a Langmuir−Blodgett deposition. Of particular interest is the fact that these surfaces, when fully covered by −OH groups, are capable of forming overlayers of *n*-alkylsiloxane films, and this phenomenon has been the basis of strategies to build up multilayer assemblies.[19]

In the present paper, we show that a set of mixed composition OH-/CH_3-terminated *n*-hexadecanethiolate surfaces can be used as substrates for the preparation of a set of ODS films with structures which correlate strongly with the changes in the wetting character of the underlying OH/CH_3 surfaces. Increasing the OH content of the substrate film surface from 100% CH_3 to ~75% OH/25% CH_3 produces monotonically increasing coverages of a series of overlayer ODS films with coexisting ordered and disordered phases until, in the region of ~80−90% OH/20−10% CH_3 content, the overlayer films change to uniformly highly organized structures with a chain organization *incommensurate* with the underlying *n*-hexadecanethiolate lattice. These data provide strong confirmation of a Langmuir-type mechanism in the formation of *n*-alkylsiloxane films under typical preparation conditions and demonstrate a method for preparation of smoothly varying controlled molecular structure films by control of substrate surface wettability, a concept which extends far beyond the specific set of OH/CH_3 mixed monolayer surfaces used in this study.

2. Experimental Section

2.1. Materials. The thiols, $HS(CH_2)_{15}CH_3$ (TCH_3; Aldrich, St. Paul, MN) and $HS(CH_2)_{16}OH$ (TOH; gift from Pharmacia AB, Uppsala, Sweden), were purified by vacuum distillation and recrystallization, respectively. Single-crystal silicon wafers were gold coated[20,21] by vacuum deposition (pressure ≤ 3×10^{-7} Torr) of a 9 nm adhesion layer of Cr followed by a 200 nm film of Au (99.999%). Octadecyltrichlorosilane ($CH_3(CH_2)_{17}SiCl_3$, OTS; Aldrich, St. Paul, MN) was vacuum distilled (7.5×10^{-2} Torr/~155 °C) immediately prior to each use. Hexadecane (Aldrich Gold Label, 99.99+%) was dehydrated by agitating an ~1:1 (v/v) mixture with sulfuric acid in a standard separatory funnel. The mixture was allowed to stand for 30 min, after which the hexadecane was decanted off and immediately chromatographed over activated alumina (Aldrich grade II). The above procedures were repeated for each set of silanizations just prior to preparation. Water for substrate cleaning was purified (Milli-RO, Milli-Q purification system; Millipore, Bedford, MA) in order to deionize (>18 MΩ cm resistivity) and remove organic impurities. All other solvents were reagent grade quality (Aldrich) and used as received.

2.2. Sample Preparation. Freshly deposited gold substrates were quickly examined by null ellipsometry (see below) and then directly immersed into ethanolic solutions of mixtures of TCH_3 and TOH. The solutions were prepared by mixing weighed proportions of the two thiols and diluting with pure ethanol to achieve a final total concentration of thiol of $\sim 1 \times 10^{-3}$ M. The mole fraction of TOH in solution, defined as $\chi_{OH} = [TOH]/([TOH] + TCH_3])$, was varied between 0.0 and 1.0 in steps of 0.125 (±0.005) M, thus giving nine data points over the entire composition range. All results presented in later sections are given in terms of the approximate surface compositions, f_{OH}, for which XPS calibrations (next section) show $f_{OH} \sim \chi_{OH}$. All thiol solutions were prepared in containers (polypropylene, Teflon, and/or glass) which were cleaned thoroughly prior to use with sequential multiple water and ethanol rinses followed with drying from a stream of nitrogen. After 4 days immersion, the samples were withdrawn from the solutions, washed extensively in ethanol, ultrasonicated in $CHCl_3$, and spun dry on a standard wafer spinner. After characterization (see below), it was found necessary to store the TOH-containing monolayers in a polar liquid, either water or ethanol,[22] until use in order to preserve the initial wetting properties and ensure reproducible *n*-octadecylsiloxane (ODS) film preparations. Without solvent immersion, the wetting was noted to change by a significant extent, particularly for $f_{OH} \gtrsim 0.50$, with prolonged ambient exposure (for example, the water contact angles of the pure TOH surfaces were found to increase from below 10° to ~30° after 12 h storage). Exposure to ambient conditions during characterization (e.g., by ellipsometry) was kept to a maximum of 60 min, after which the samples were reimmersed in the storage liquid for a maximum of 5 h before silanization. Just prior to silanization, all samples were rinsed extensively with *n*-hexane and ethanol, ultrasonicated in $CHCl_3$, and spun dry. Finally the films were covered with low organic content, deionized water, spun until the surface was dry to the eye, and then immediately immersed in the reaction solution. The water treatment was found to be essential for reproducible synthesis of subsequent alkylsiloxane monolayers,[13,23] as shown by extremely erratic ODS coverages observed on all non-prehydrated surfaces. The silanization solution consisted of a 70:30 mixture of $C_{16}H_{34}/CCl_4$ containing 2.5×10^{-3} M OTS and was maintained at 20.0 ± 0.2 °C in covered glass containers which were precleaned with freshly prepared chromosulfuric acid followed by exhaustive pure water rinsing and oven drying. The ambient environment over the silanization reactor was not controlled but consistently measured ~30% relative humidity. After 15 min immersion the wafers were withdrawn from the solution, ultrasonicated in ethanol for 5 min, washed extensively in separate pure $CHCl_3$, CCl_4, and ethanol solvents, and finally spun dry. After these reaction times, the silanized samples were observed to emerge oleophobic and autophobic. However, the rate of *dewetting* of the solution mixture was noted by eye to increase systematically as the hydroxyl content of the thiolated substrates increased. The stability of RS layers during the ODS deposition was demonstrated by cycling thiolate monolayers through the silanization process except for the absence of OTS. The effects of the latter treatment showed no measureable changes on the original ellipsometric, contact angle, and infrared spectroscopic data. Finally, we note that multiple samples were made and characterized, at least two at each desired composition.

2.3. X-ray Photoelectron Spectroscopy Determination of Composition. The connection between the solution compositions, χ_{OH}, and the actual compositions of the mixed monolayers was determined by XPS analysis of a subset of multiple (two to four) samples of five different compositions (plus the pure monolayers). The fraction of TOH present in the mixed monolayer was determined as the oxygen atom composition, χ_O, using the equation

$$\chi_O = [A_{(O)MM}]/[A_{(O)OH}] \quad (1)$$

where $A_{(O)MM}$ and $A_{(O)OH}$ are the normalized (to Au 4f intensity as sum of 7/2 and 5/2 peaks) integrated areas of the O 1s peaks (532 eV) in the mixed and pure TOH monolayers, respectively. No O 1s signals were detected above the noise for the TCH_3 films. For unsilanized thiolate films the S 2p intensities were too weak relative to instrument noise to provide reliable measures of coverage. Observed values of χ_O at representative χ_{OH} are, respectively, 0.14(±0.033), 0.10; 0.205(±0.040), 0.25; 0.46(±0.038), 0.50; 0.69(±0.031), 0.75; and 0.93(±0.01), 0.90.

These data show that χ_O tracks the solution composition within a maximum experimental error range of ±0.06 mol fraction of OH with ±0.04 as a representative range. The error statistics include both multiple analyses and multiple samples. A similar XPS analysis has been reported for mixed monolayers of $S(CH_2)_{10}CH_3$ and $S(CH_2)_{11}OH$ on gold,[24] and the observed surface and solution OH compositions are in agreement with the present ones within a maximum range of ~0.1 mol fraction. On the basis of the calibration runs above, for all subsequent monolayer preparations the surface fraction of OH groups, defined as f_{OH}, was set equal to the value of χ_{OH} for the preparation solution. The separate designation f_{OH} is used in order to signify that the calibration errors are to be associated with these compositions, as opposed to χ_O values, which are precisely known from the preparation procedure. In general, when necessary to reflect the experimental uncertainties in later discussions, the f_{OH} values are conservatively rounded off to the nearest decimal.

2.4. Ellipsometry Characterization of Film Thicknesses. *2.4.1. Measurements.* Single-wavelength (632.8 nm) measurements were done using a null-ellipsometer (Rudolph AutoEL-II, Fairfield, NJ) operating at a 70° angle of incidence. For each sample preparation, the polarization parameters,[25] Δ and Ψ, were measured at five arbitrarily chosen spots on the freshly cleaned gold substrates, thiolated substrates, and the final silane-treated, thiolated substrates. The instrumental precision was 0.04°, and the overall, sample-to-sample errors in terms of final calculated film thicknesses are within ±1 Å. The single-measurement time was ~1 min, and the complete set of measurements for each bare substrate were minimized to within 10 min after precleaning in order to reduce the chances of adventitious contaminant adsorption or any surface reorganization of the OH groups.[22]

2.4.2. Film Thickness Calculations. 2.4.2.1. Assignment of Dielectric Functions. Thicknesses were calculated from Δ and Ψ using a generalized model of parallel, homogeneous layers with anisotropic optical functions in which the layers are separated by sharp, planar interfaces. The optical functions (refractive index or dielectric constant) of the film-free gold substrates were derived from the Δ and Ψ values of freshly evaporated gold films using a two-phase Au/air model and subsequently applied to film thickness calculations using air/RS/Au and air/ODS/RS/Au models.[26] Film anisotropy was included in order to account rigorously for the effects of alkyl chain orientation in the cases where the chains appeared to adopt nearly all-*trans* conformations and assume uniform tilts from the surface plane. Diagonalized refractive index tensors[27] expressing the anisotropy were obtained from den Engelsen's calculations[28] for dense assemblies of all-*trans* extended polymethylene chains; for the alkanethiolate and ODS chains with 15 and 17 CH_2 units, respectively, values[28] of $n_\perp = 1.481$ and $n_\parallel = 1.557$, 1.484, and 1.559, respectively, were used. For the alkanethiolate films, known to be tilted at ~30°,[3] comparisons with isotropic film model simulations using a refractive index tensor collapsed to a scalar value of 1.506 (=(1/3)($2n_\parallel + n_\perp$)) showed that the isotropic approximation overestimates the calculated film thickness relative to the anisotropic values for ~30° chain tilts by ~0.8 Å, a value within the ±1 Å experimental uncertainty. Similar calculations for models of ODS/RS/Au films showed that the isotropic approximation leads to overestimation of the total film thicknesses (ODS + RS) relative to the anisotropic model by ~1.8 Å.

2.4.2.2. Selection of Calculation Models. The anisotropic four-phase model (air/ODS/RS/Au) was used for the thickness calculations of the highest coverage composite films. However, for the low-coverage films, where intermediate conformational disorder of the ODS alkyl chains is observed (see section 3.4.1), the rigorous anisotropic model was used for the RS underlayer, while two different limiting models were used for the ODS overlayer: (1) a heterogeneous film with 26.2 Å thickness domains of densely packed all-*trans* molecules separated by void regions of volume fraction v_i and (2) a completely liquid-like assembly with a scalar refractive index of 1.44, appropriate for a liquid *n*-alkane. In the first approach, the refractive index tensor was calculated using the value assigned to the densest ODS monolayers (see above) but modified using the Maxwell-Garnett (MG) approximation.[29] Agreement between experimental and observed Ψ and Δ values sets a value for v_i which allows calculation of an average film thickness defined as $26.2v_i$ (Å). In the second approach, the ellipsometric film thicknesses were calculated using a standard four-phase isotropic model in the Ψ, Δ simulations.

2.5. Contact Angle Measurements. Advancing and receding contact angles were measured using a Ramé-Hart Model 100 contact angle goniometer using the sessile drop and captive drop methods. The samples were placed in a chamber maintained at 20.0 ± 0.5 °C and saturated with the vapor of the test liquids. Flat-tipped syringes were used to deliver controlled volume drops to the sample surface. The volume of the test liquid held between the syringe tip and the surface was slowly changed while keeping a constant area of sample−liquid interface. The maximum value of the advancing contact angle was measured at the highest volume, and conversely, the minimum value afforded the measurement of receding angle. Hexadecane and water were used as probe liquids. Five measurements of the advancing contact angles and the associated hysteresis were made for each sample surface.

2.6. Infrared External Reflection Spectroscopy. Quantitative reflection spectra were collected using an air (CO_2, H_2O free) purged, custom-modified Digilab FTS-60 Fourier transform infrared spectrometer (Bio-Rad, Cambridge, MA). The incoming infrared radiation was focused on the sample with an ~*f*/20 beam at an 86° angle of incidence and the reflected beam detected using a narrow band MCT detector cooled with liquid nitrogen. A wire-grid polarizer was placed immediately before the sample and oriented to give *p*-polarization. The final spectra were obtained by coadding multiple scans collected at 2 cm^{-1} resolution with a mirror velocity corresponding to a data collection rate of 10 kHz. The interferograms were Fourier transformed with triangular apodization and zero-filling. For quantitative determination of peak frequencies the interferogram zero-filling was enhanced to increase the point density by a factor of 6.[30] The spectral intensities are reported as reflectivities in absorption units, $-\log(R/R_0)$, where R_0 is the reflectivity of a reference sample prepared by freshly cleaning an evaporated gold substrate using a UV-ozone cleaner (Model uvc-100, Boekle Industries, Philadelphia, PA).

3. Results

3.1. Ellipsometry. *3.1.1. Initial Alkanethiolate Monolayers.* The ellipsometric film thicknesses of unsilanized, RS/Au samples are nearly constant between 19 and 21 Å, with a slight monotonic trend toward higher values with increasing f_{OH}. Accounting for the slight differences in assigned scalar refractive index values in the present and earlier reports,[31] the thickness values of the pure TCH_3 and TOH films are identical, within experimental errors, with published values. The presently observed thickness vs f_{OH} trend implies that the mixed monolayers possess overall coverages and structural characteristics

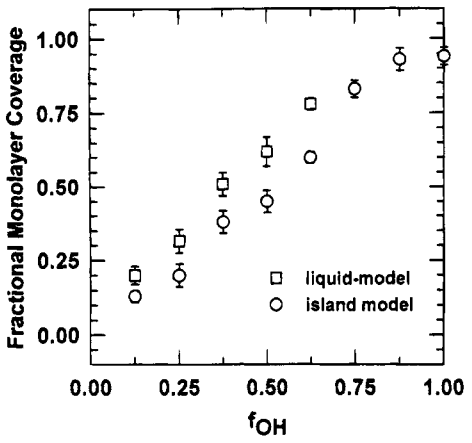

Figure 1. Ellipsometrically determined ODS coverages on mixed composition hexadecanethiolate monolayers on Au as a function of f_{OH}. The coverages were calculated using two models: homogeneously disordered, liquid-like chains (□) and heterogeneously distributed islands of ordered chains (○). See text for details.

identical to those of the pure monolayers except for the differing terminal functionality.

3.1.2. Silanized Composite Films. Since all of our data, particularly the infrared spectra (section 3.3), indicate no perturbation of the underlayer *n*-alkanethiolate film by an ODS overlayer, the ODS overlayer coverages were extracted from the ellipsometry data by assuming that the thiolate underlayer thicknesses were equal to those in the unsilanized films. The coverages were calculated from the ellipsometric thicknesses, d_e, as d_e/d_0, where d_0 is 26.2 Å, the estimated length of an all-*trans* ODS chain.[32] In combination with the assignment of the film refractive index value to that of crystalline polyethylene, the 100% coverage model would correspond to an ideal monolayer of ODS chains oriented perpendicular to the substrate surface plane and packed with 5.42 chains nm^{-2}, the corresponding chain density on the *a,b* plane of a polyethylene crystal.[33] The results, based on both the four-phase isotropic and anisotropic models (see section 2.4.2), are given in Figure 1. At high f_{OH} ($\gtrsim$0.85−0.90), where the coverages approach a complete monolayer, the anisotropic, island-like model with dense-packed, oriented chains is appropriate and the anisotropic model value of ~94(±3.0)% is assigned to the coverage. This value corresponds within experimental errors to the values of 86−93% determined for the highest coverage ODS films on SiO_2 prepared in exactly the same way as the present films[13b] and to the values of ~94.0(±1) and 85.5(±9)% determined for dense films on SiO_2 from grazing incidence X-ray diffraction[34] and X-ray reflectivity measurements,[32] respectively. At intermediate values of f_{OH}, neither model is, *a-priori*, an accurate representation of the actual film structures, but the actual coverages should be bounded between the two limiting values. Despite this uncertainty, Figure 1 shows an unambiguous monotonic decrease of coverage with decreasing f_{OH}. Finally, at f_{OH} = 0, the ODS coverage is consistently 0 within experimental error.[35]

3.2. Wetting. *3.2.1. Initial n-Alkanethiolate Monolayers.* Figure 2 shows plots of advancing water and hexadecane contact angles (θ_w and θ_{HD}, respectively) against f_{OH} for the initial unsilanized substrates. At f_{OH} = 0, excellent agreement of θ_w is observed with the value of 114° reported for a dense-packed pure methyl surface.[36] As f_{OH} is increased, θ_w decreases monotonically to the limiting range of 4−14° (maximum sample-to-sample variation at these low angles). A variety of studies give values for pure OH-terminated surfaces ranging

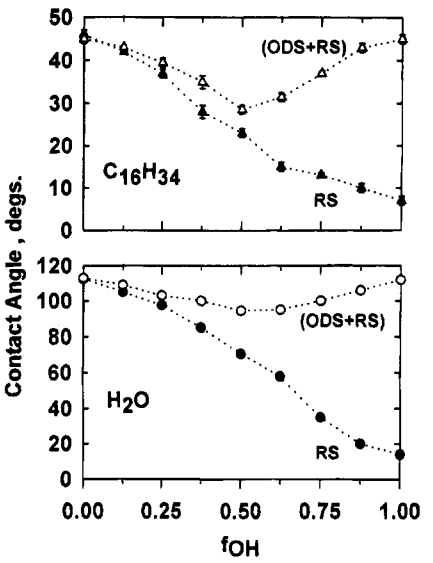

Figure 2. Water and hexadecane advancing contact angles for mixed composition hexadecanethiolate monolayers on Au substrates and for ODS-coated (silanized) mixed alkanethiolate monolayers as a function of f_{OH}.

from less than 10° to as high as 42°.[22,36−38] Our observed sample-to-sample scatter in θ_w for values above ~10° were all within ±1.5°. Hexadecane contact angles show a monotonically declining dependence on f_{OH}, with a maximum value of 46° at f_{OH} = 0 and a minimum value range of 4−14° at f_{OH} = 1.0. The maximum values are in good agreement with those noted for the pure CH_3 surfaces of monolayers of ODS on SiO_2 substrates[12−15] and the pure TCH_3 films (see above). A previous study[17] of $CH_3(CH_2)_{11}SH/HO(CH_2)_{11}SH$ mixed monolayers on gold reports a similar monotonic increase in θ_{HD} with increase in OH content, but, in addition, this study reports a distinct environment-dependent kink in θ_{HD} at 30−45 and 70% OH for measurements made at 30 and ≤2% humidity, respectively. However, in comparison, our data for the longer C_{16} chains, taken with 0.125 steps in f_{OH}, do not resolve such kinks under our specific wetting conditions of uncontrolled ambient humidity and saturated hexadecane vapor, conditions deliberately selected to mimic the ODS preparation conditions.

3.2.2. Silanized Composite Films. After silanization, the surfaces become quite hydrophobic and oleophobic with θ_w > 96° and $\theta_{HD} \gtrsim 29°$ for all f_{OH} values (Figure 2). At f_{OH} = 1.0 and 0, the θ_w and θ_{HD} values correspond almost exactly to those of pure CH_3 (ODS and TCH_3) surfaces,[12,15,36] while in the midregion of $f_{OH} \sim 0.5$, the minimum values of θ_w and θ_{HD} drop below and remain above the corresponding respective values of ~102°[39] and ~0−10° observed for pure CH_2 (polyethylene) surfaces. These trends indicate the appearance of CH_2 groups at the surface at intermediate f_{OH} values and thus signal the corresponding appearance of conformationally disordered alkyl chains. Since θ_w^{min} is less than the pure CH_2 value of 102°, the wetting surfaces for these midregion films must include some fractions of exposed polar OH groups and/or $SiO_x(OH_y)$ groups located at the RS/ODS interface. These data indicate that some spots in these maximally disordered ODS films must be no thicker than 5−10 Å, the general screening length of the wetting effect.[40] Since a pure CH_2 surface is fully wet by hexadecane, $\theta_{HD}^{min} \sim 29°$ signals the existence of a strongly disordered chain structure presenting *both* CH_2 and CH_3 groups at the film surface.

3.2.3. Estimation of Effective Surface Compositions. The above qualitative discussion of surface (outer 5−10 Å region)

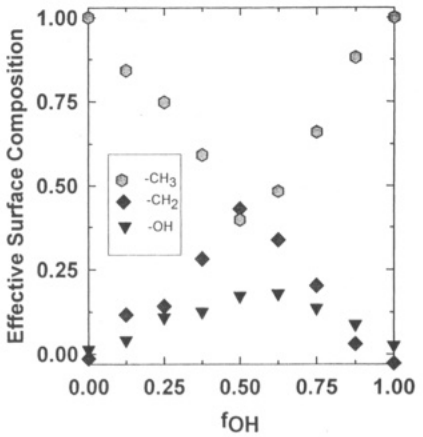

Figure 3. Effective surface group compositions of silanized thiolate samples as a function of f_{OH}. The surface compositions were estimated from the measured water and hexadecane contact angle data (Figure 2) using eq 2. See text for details.

composition can be put on a numerical basis using the simple approximation[41]

$$\cos(\theta_{mix}) = \sum[f_i \cos(\theta_i)] \quad (2)$$

where θ_{mix} and θ_i are the equilibrium contact angles of the mixed composition surface and the pure surface of the ith component, respectively, and f_i is the effective mol fraction of the ith surface component. These values of f_i are to be regarded as a transformation of the wetting data, not necessarily equal to the true surface composition, such as might be found spectroscopically.

Using eq 2 with measured contact angles for the pure surfaces, the effective surface compositions of CH_2, CH_3, and OH functional groups (including both $-CH_2OH$ and $\equiv$SiOH with the assumption that $\equiv$SiOH groups behave like hydrated SiO_2 surfaces) were calculated. The results shown in Figure 3 reveal several salient structural features of the ODS film surface. First, at $f_{OH} = 0$ and 1.0, dense, essentially pure CH_3 surfaces are observed. In the case of the near-complete coverage (Figure 1) $f_{OH} = 1.0$ film, the data indicate that the surface defects associated with the (6 ± 3)% coverage deficiency do not expose the interior of the film to the wetting liquid. This conclusion indicates that the defects are not macroscopic patches, consistent with several theoretical studies which have pointed to the insensitivity of wetting to small fractions of line (and point) defects.[42] For films with $0 < f_{OH} < 1.0$, the analyses indicate that significant fractions of CH_2 groups are exposed at the film surfaces together with limited fractions of OH groups of the underlying thiolate layer. These data imply partial coverages with a dependence of conformational defect content on f_{OH}. The observation of a maximum in the CH_2 group ($\sim$40%) exposure at $f_{OH} \sim 0.5$ leads to the conclusion that the midcomposition films possess the maximum conformational disorder with the most extensive chain folding.

3.3. Infrared Spectroscopy. *3.3.1. Experimental Observations.* Spectra of the C−H stretching modes in the region 2700−3100 cm^{-1} were used to characterize the average conformational ordering, average chain tilt angles, and compositions of the films. Spectra in the low-frequency region, $\sim$750−1500 cm^{-1}, which contain contributions from siloxy network modes (for ODS overlayers) and polymethylene chain modes, were used to characterize the structures of the siloxy networks, chain conformational ordering, and chain organization. The lack of observed changes[35] in the $f_{OH} = 0$ spectra indicates inertness of the pure CH_3 films to ODS deposition.

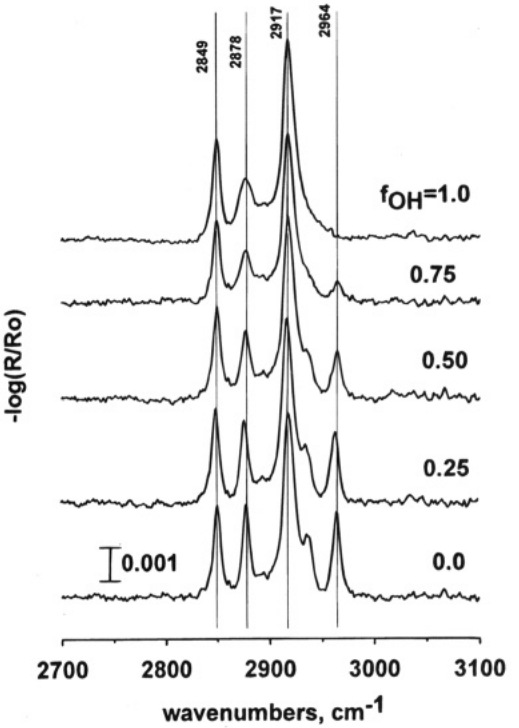

Figure 4. p-polarized, infrared external reflection spectra at an 86° incidence angle in the 2700−3100 cm^{-1} frequency range for initial unsilanized, mixed composition hexadecanethiolates on Au. Data are shown for a set of selected values of f_{OH}.

3.3.1.1. C−H Stretching Mode Spectra. Spectra of the C−H stretching mode features for selected initial RS films are presented in Figure 4. The uncorrected (no scaling factors) difference between the final (RS/ODS) composite film (ODS+RS) spectra and their corresponding initial RS film spectra is presented in Figure 5. The extreme stability of the initial thiolate monolayers against solvent damage, demonstrated specifically by the constancy of the infrared spectra after extensive solvent exposures and ultrasonic treatment in ethanol, supports our presumption that the major features of the RS film spectral response are effectively unchanged by an ODS overlayer, and thus the ODS spectral contributions of each sample are effectively isolated by the corresponding difference spectrum. Table 1 summarizes relevant vibrational mode assignments for these films.

The spectra collected for the unsilanized thiolate monolayers are in good agreement with the earlier reports of single[31] and mixed component[43] monolayer spectra. A detailed study of the structural interpretations of the IR spectra of these mixed n-alkanethiolate monolayers will be reported separately.[44] Here, we only summarize several spectral features as a prelude to the detailed discussion below. First, as f_{OH} is increased, Figure 4 shows that the integral intensity of the methyl asymmetric mode (r^-) peak at 2964 cm^{-1} diminishes. Further, the integrated absorption of this peak correlates approximately linearly with the f_{OH} values, an indication of the usefulness of the r^- peak for quantitating the monolayer composition in these particular films.[45] Second, a comparison of the peak frequencies of the symmetric (d^+) and antisymmetric (d^-) methylene stretching mode absorptions (2849.6 ± 0.3 and 2917.8 ± 0.4 cm^{-1}) with those for crystalline (typically 2850 and 2916 cm^{-1})[46] and liquid n-alkanes (2854−2856 and 2924−2928 cm^{-1})[47] of comparable chain lengths suggests that the observed peak frequencies in the films correspond well to those of highly conformationally ordered chains in a crystalline-like environment. This picture is further supported by the narrow line widths of the d-mode

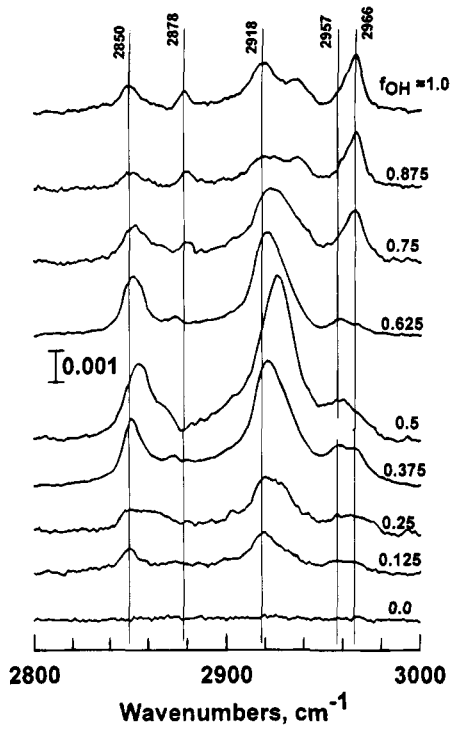

Figure 5. Residual ODS infrared spectra in the 2700−3100 cm^{-1} frequency range for silanized, mixed composition hexadecanethiolates on Au for a set of selected values of f_{OH}. The residual ODS spectra were obtained by subtracting the initial thiolate spectra (Figure 4) from the composite (ODS+RS) spectra (not shown); no scaling factors were used in the subtractions.

features, *viz.*, ~8−10 cm^{-1} for d^+ modes and 11−14 cm^{-1} for d^- modes, which are close to typical values of 7−10 and 10−13 cm^{-1}, respectively, obtained from the spectra of corresponding bulk crystalline compounds and similar chain length bulk *n*-alkanes.[31,48] For these purposes, the line widths were measured by a very approximate curve-fitting routine for which the absorptions at ~2849 and ~2917 cm^{-1} were fitted by single peaks.

In contrast to the initial RS film spectra, the ODS residual (difference) spectra (Figure 5) show quite discernible variations in peak frequencies, line widths, and intensities with f_{OH}. The lack of features above the noise in the $f_{OH} = 0$ films corresponds to ≤2 Å thickness for any ODS adsorption.[35]

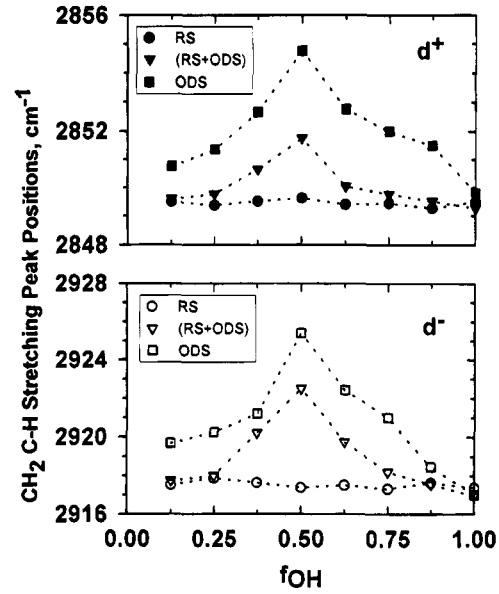

Figure 6. Variation in peak frequency positions for methylene symmetric (d^+) and antisymmetric (d^-) C−H stretching mode vibrations, as functions of f_{OH}. Data are shown for the initial thiolate (RS) monolayers (○), final silanized thiolate (RS+ODS) monolayers (▽), and the residual ODS (difference) spectra (□).

Figure 6 summarizes the dependencies of the d^+ and d^- mode peak frequencies on f_{OH} for the spectra of the initial alkanethiolate monolayer (Figure 4), the composite (ODS+RS) film (Figure 5), and the residual ODS film (difference spectrum, Figure 6). While the d^+ and d^- peak frequencies of the initial thiolate monolayer spectra are constant at 2849.6(±0.3) and 2917.4(±0.5) cm^{-1}, respectively, the values for the composite and the residual ODS film spectra follow a convex-shaped curve with maxima at $f_{OH} \sim 0.5$. The residual ODS film spectra show minimum d^+ and d^- values of 2849.5 and 2916.8 cm^{-1}, respectively, and maximum values of 2854.6 and 2926.1 cm^{-1}, respectively. These results indicate that the average conformational ordering of the chains in the ODS films is highest at $f_{OH} = 1$, with the maximum disorder arising near $f_{OH} \sim 0.5$. This trend agrees remarkably with the one drawn from the wetting data (see section 3.2.2 and Figure 3).

Figure 5 also shows significant changes in the line shapes of the d^+ and d^- peaks with f_{OH} values. These changes are not

TABLE 1: Reported Assignments of Selected Vibrational Modes of Alkyl Chains and Siloxy Groups in *n*-Alkylsiloxanes

mode assignment[a,b]	approximate peak frequencies, cm^{-1}[a] bulk cryst. alkane	liq. alkane	$C_{16}H_{33}SH$/Au
CH_3, asym. str., op (r_a^-)	2962		2965
CH_3, asym. str., ip (r_b^-)	2952	~2957	~2958
CH_2, asym. str. (d^-)	2915	2928	2919
CH_3, sym. str. (r^+)	2870		2878
CH_2, sym. str. (d^+)	2846	2856	2851
CH_2, scissors, def. (δ_{CH_2})	1473.6, 1461.8	1467	1468
CH_3, sym. def. (δ_{CH_3})		1374.5	1383
CH_3 wag, *end-gauche* (*gtt*) CCC sequences		1342, 1345	
CH_2 wag, *kink* (*tgtg*t*) CCC sequences		1306, 1312	
CH_2 wag, *trans* (*ttt*) CCC sequences, prog. series	1330, 1317, 1298, 1280, 1262, 1245, 1228, 1207, 1196		~1349, 1326, 1306, 1282, 1263, 1244, 1223, 1205, 1183

mode assignments[a,b]	approximate peak frequencies $[C_8H_{17}SiO(OH)]_6$	$[C_7H_{15}SiO(OH)]_6$	$[C_6H_{13}SiO(OH)]_6$
Si−OH str./bend	900	980	890
Si−O−Si str.	1130	~1140−1185	1075−1100

[a] Based on the data reported previously for hexadecane and octadecane bulk polycrystalline material[62] and hexadecanethiolate on gold.[27] Si−O mode features were derived from the infrared transmission spectra reported for bulk, hydrolyzed samples of *n*-alkyltrichlorosilanes.[50] [b] Abbreviations used: str. = stretch; asym. = asymmetric; sym. = symmetric; op = out of plane; ip = in plane; def. = deformation; prog. = progression.

straightforward to interpret quantitatively,[49] especially in the case of the d^- peak, where overlapping with a Fermi resonance mode of the r^+ peak at ~2931 cm^{-1} occurs, but an important observation is that the line shapes at the intermediate f_{OH} values do *not* conform to those observed in spectra of *n*-alkyl chains in either the pure bulk crystalline or pure liquid states. Rather, they appear to correspond to states of average partial conformational disorder, for which two extreme models are possible: (1) a single, uniform phase of partially disordered chains or (2) a heterogeneous structure of coexisting phases of highly disordered chains and all-*trans* extended chains. The validity of the heterogeneous model was supported by the observation that these complex line shapes could be fit quite closely by superposition of two components, a narrow, lower frequency component due to conformationally ordered chains and a broader, higher frequency peak due to conformationally disordered chains. The component characteristics were approximated by analyzing the spectra collected in an independent study of bulk phases of pure OTS and hydrolyzed OTS, which are in liquid and crystalline states, respectively.[50] Details of the fitting procedure are deferred until the section on simulations (section 3.3.2).

The intensities of the d^+ and d^- bands of the residual ODS spectra (Figure 5) show striking changes as functions of f_{OH} as compared to the relatively constant values observed for the unsilanized thiolate monolayer spectra (Figure 4). Of special note is the singularly large intensity value in the vicinity of f_{OH} ~ 0.5 for the ODS films. Peak intensities are regulated by coverage, molecular orientation, and the intrinsic values of the transition dipole moment of the specific vibrational mode in question. It is clear that the observed intensity maximum does not signal a point of maximum coverage since the ellipsometric data in Figure 1 definitively establish that the coverages are well below maximum at this point. Evidence presented below (section 3.3.2) suggests that orientational changes of the CH_2 groups are responsible for the intensity maximum.

The symmetric (r^+) and asymmetric (r^-) C−H stretching modes of the CH_3 groups appear at ~2878 and ~2963 cm^{-1}, respectively, in Figures 4 and 5. The r^+ mode is complicated by the presence of overlapping contributions from a d^+ mode Fermi resonance[46c] peak and a poorly characterized peak, tentatively assigned to the terminal CH_2 group of the OH-terminated alkanethiolate molecules[51] (see Figure 4). For this reason, the r^+ peak was not analyzed for structural implications. However, useful information was obtained from the r^- mode. Figure 5 shows that the residual ODS r^- peak frequencies are constant at ~2966 cm^{-1} for f_{OH} > ~0.75 while below ~0.75 a second component at ~2957 cm^{-1} arises, and this latter component appears weakest for the f_{OH} ~ 0.5 film. For comparison, we note that a broad singlet at 2956 cm^{-1} with a line width of 11−14 cm^{-1} is observed for bulk liquid OTS, a typical result for liquid-state alkyl chains.[50] The higher peak values of ~2966 cm^{-1} observed for f_{OH} > ~0.75 are consistent with the values of 2964−2966 cm^{-1} obtained in the spectra of *n*-alkanethiolates on gold[31,44] (see Figure 4) and *n*-hexadecanoic acid on oxided aluminum,[52] highly organized monolayers for which the terminal methyl groups experience dense packing at the air/film interface. On this basis, the simplest average chain structure for the high-range f_{OH} films is one in which a major fraction of the alkyl chains exhibit a dense-packed extended, high *trans* conformation chains. However, in the case of lower f_{OH} films, the appearance of the doublet peaks implies coexisting disordered and ordered chain phases. At f_{OH} ~ 0.5 the r^- peak emphasizes the low-frequency component and appears to exhibit the general line shape for a bulk liquid. This observation can be reconciled with a film structure for which a dominant fraction of the CH_3 groups experience low-density packing and are attached to conformationally disordered chains.

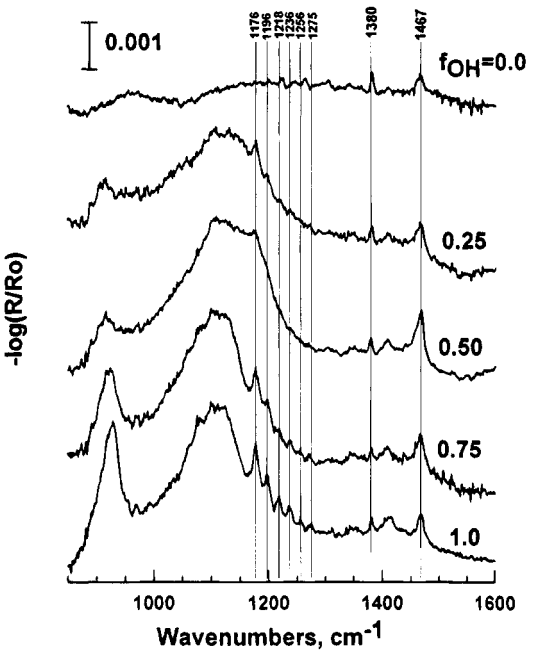

Figure 7. p-polarized, infrared external reflection spectra at an 86° incidence angle in the low-frequency range (850−1500 cm^{-1}) for final silanized thiolate (RS+ODS) monolayers. Data are shown for a set of selected values of f_{OH}.

3.3.1.2. Low-Frequency Region: Siloxane Network Modes and Alkyl Chain Modes. Figure 7 shows the observed raw (ODS+RS) spectra in the low-frequency region for selected composition films. The major spectral features of interest arise from siloxane group modes and polymethylene chain wag−twist modes, both unambiguously associated with the ODS films since the spectra of the initial, unsilanized samples (not shown above) show no spectral features of comparable intensities at the same frequencies in this region. The interpretation of structural features from each mode is discussed in turn below, starting with the siloxane modes. Note that the f_{OH} = 0 spectrum essentially represents that of a pure *n*-alkanethiolate film (see previous section).

For all f_{OH} > 0 values, two intense, broad peaks centered at about 924 and 1080 cm^{-1} are observed. Similar spectral features in this region have been reported for bulk poly(alkylsiloxanes),[53,54] for example, as observed with the hydrolysis products of bulk hexyl- and octyltrichlorosilanes.[53] On the basis of the mode assignments reported in the above studies, the peak observed at ~924 cm^{-1} is assigned to an Si−OH stretching and/or SiO−H bending mode and the broader peak at ~1080 cm^{-1} to the Si−O−Si antisymmetric stretching mode.[54,55]

The integrated, base-line-corrected intensities of these peaks are shown in Figure 8, where it is observed that the 924 cm^{-1} SiOH stretch/bend mode peak intensity increases monotonically with increasing f_{OH} values, whereas the 1080 cm^{-1} SiOSi stretching mode peak intensities follow a convex pattern, with a maximum at f_{OH} ~ 0.5. A quantitative measure of the relative changes is given conveniently in the form of the integrated intensity ratio, I_{SiOSi}/I_{SiOH}, which is seen to decrease with increasing f_{OH}. While it is not possible to interpret these changes in detail,[56] one broad assumption which appears reasonable is that the general chemical bonding character of the SiOH and SiOSi units does not change with f_{OH}. On this basis, the transition dipole moment *magnitudes* can be assumed constant

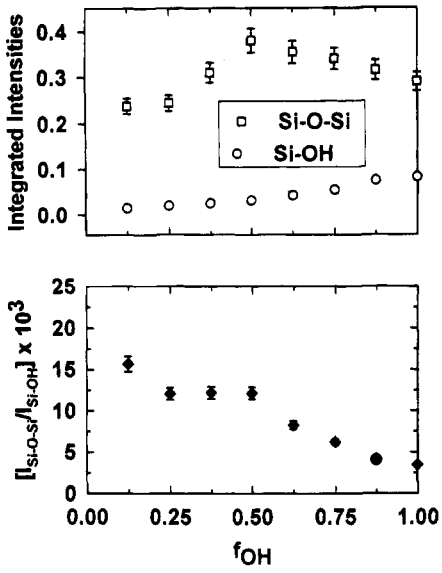

Figure 8. (top) Observed variations in integrated intensities of the peaks assigned to Si−OH bending and Si−O−Si stretching mode vibrations as functions of f_{OH}. (bottom) Ratio of integrated intensities, $I_{Si-O-Si}/I_{Si-OH}$, as a qualitative measure of the degree of siloxy group cross-linking (see text for details).

and the changes in the integrated band intensities with f_{OH} thus assigned to a combination of changes in bond reorientations and degree of cross-linking of the siloxy network. Further, the decrease in the I_{SiOSi}/I_{SiOH} values with increasing f_{OH} suggests that the degree of cross-linking in the siloxy network decreases with increasing f_{OH}.

With increasing value of f_{OH}, both the 928 and 1080 cm^{-1} peaks become gradually narrower and better defined. Some understanding of this behavior can be obtained by comparison with the results of previous studies of the hydrolysis of methyltrichlorosilanes. The major hydrolysis products are cyclic trimers and tetramers,[54] namely, $[H_3CSiO(OH)]_x$, with $x = 3$ or 4, for which the spectra have been reported[54] to show a splitting of the Si−O−Si stretching mode peak into components at ~1020 and 1090 cm^{-1}, respectively. In contrast, linear structures with a $[H_3CSiO(OH)]_x$ sequence generally are reported to exhibit[55] a well-resolved doublet of peaks at 1020 and 1080 cm^{-1} for cases of $x > 2$. On this basis, the observed single broad peak with a plateau of maximum intensity between 1040 and 1080 cm^{-1} in Figure 7 is consistent with the formation of cyclic oligomers with a dominant population of tetramers ($x \geq 4$) and a minor presence of trimers ($x = 3$). Further, previous infrared spectroscopy studies[57] of bulk-phase and surface silicon dioxide layers have shown that a narrowing of the Si−O−Si antisymmetric stretching mode peak correlates with increased structural order, *viz.*, a narrower distribution of Si−O−Si bond angles and Si−O bond distances. Applying this correlation to the present case leads to the conclusion that the structural order of the siloxy network should be highest at high f_{OH} values.

Starting on the high-frequency tail of the 1080 cm^{-1} siloxane mode peak, a series of peaks are observed between 1170 and 1380 cm^{-1} for the $f_{OH} = 1$ substrate, as shown in Figure 7. The features weakly appear for $f_{OH} = 0.75$, disappear for $f_{OH} = 0.5$ except for the initial peak in the progression at 1175 cm^{-1}, and reappear as weaker vestiges of the strongest members of the series in the $f_{OH} = 0.25$ monolayers. The observation of band progressions in this spectral range for solid-phase alkyl compounds is attributed to coupled CH_2 wag modes of the alkyl chain, with the strongest intensities observed when a given chain is in an all-*trans* conformational sequence.[58] We assign these spectral features in Figure 7 to the CH_2 groups of the ODS chains,[59] and, on this basis, the data provide qualitative, but compelling, evidence for the presence of some fraction of conformationally ordered chains in the composite (ODS/RS) films.

Two features of these wagging progressions provide important structural clues about the polymethylene sequence in the ODS layer. First, it is known that the number and spacing of these modes are directly related to the length of all-*trans* sequences of the *n*-alkyl tail of the film.[60] In the case of a substituted alkane $CH_3(CH_2)_{n-m}(CH_2)_mX$, where n and m are the number of CH_2 units in the molecule and in an all-*trans* sequence, respectively, the number of wag−twist modes is equal to m and the interband spacing, $\Delta\nu$ (below ~1350 cm^{-1}), is related to m by the following equation:[61]

$$\Delta\nu = 326/(m + 1) \qquad (3)$$

A 17 wag−twist band progression is expected for a fully extended ODS chain. While verification of this number is precluded by the inherent noise in our spectra, all the spectra in Figure 7, except for the $f_{OH} = 0.5$ case, do allow measurement of reliable values of $\Delta\nu$ between 1170 and 1275 cm^{-1}. A constant value of 19.3 ± 0.3 cm^{-1} was obtained, which yields $m = 16(\pm 0.2)$ from eq 3. Thus, on average, one end CH_2 unit per chain is in a *gauche* state, or equivalently, an ~[100 × (1/17)] = 5.9% average end *gauche* population exists in the monolayer. Next, we consider the observed variations of the wag−twist intensities with f_{OH}. Figure 7 shows that all the spectra exhibit some vestiges of the wag−twist progression; in the weakest case of $f_{OH} = 0.5$ this amounts to the appearance of the band-head peak at 1175 cm^{-1}. In order to make interpretations, variations of the *gauche* conformer populations, the total chain coverage,[62] and the chain orientations must be considered. However, since the interband spacing appears constant (except in the $f_{OH} = 0.5$ case, where no value is obtainable) at a value giving a >94% *trans* conformer population, it can be concluded that the chain conformational sequences are constant with f_{OH}, except perhaps at $f_{OH} = 0.5$. This leaves the intensity variation to be explained on the basis of orientation and coverage. These factors cannot be separated directly by analyzing the wag−twist features alone, but it is clear from Figure 1 that ODS coverages drop with decreasing f_{OH} in a manner qualitatively consistent with the changes in wag−twist intensity in Figure 7. The most general conclusion to be drawn from the above analysis of these modes is that at all f_{OH} values some fraction of the ODS overlayer exists in the form of highly conformationally ordered alkyl chains.

The highest frequency feature observed in Figure 7 is the peak at 1467 cm^{-1}, which is straightforwardly assigned to the CH_2 scissoring deformation mode. For $f_{OH} > 0$, a single band is observed at 1467.5 cm^{-1} with a fwhm of 8−12 cm^{-1}. The constancy of the line width with f_{OH} implies a constant, coverage-independent packing arrangement of ODS chains. Further, these peak features (narrow bandwidths and peak positions) are in good correspondence with the CH_2 scissoring peaks obtained for triclinic or hexagonal crystalline structures of *n*-alkanes.[63] For a dense orthorhombic packing of chains, crystal field splitting creates two components observed either as a well-resolved doublet or as an asymmetric peak with a shoulder.[63] For conformationally *disordered* alkanes, the line widths generally are observed to be ~18−25 cm^{-1},[63] values significantly larger than for the corresponding ordered phases. Thus, we conclude that the CH_2 scissoring mode features support the presence of ordered ODS chains, packed in a triclinic or hexagonal type of arrangement, for films formed on substrates of all f_{OH} values.

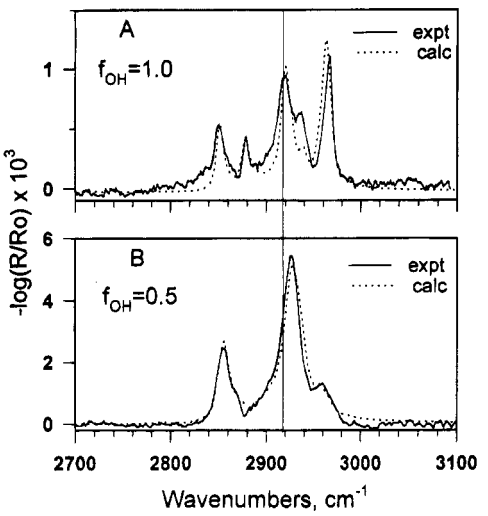

Figure 9. Comparisons of experimental and simulated residual spectra of f_{OH} = 1.0 (A) and 0.5 (B) silanized monolayers. The experimental spectra are those shown in Figure 5.

3.3.2. Spectral Simulations. Spectral simulations of the C−H stretching mode spectra were performed in order to obtain more quantitative details of the monolayer structures. Methods derived from classical electromagnetic theory[64] were used, and full details are given elsewhere.[27]

The composite film structures were modeled as consisting of four layers: air/ODS/RS/Au, with the experimental parameters as given in the experimental section. Individual layer thicknesses were assigned from the ellipsometry data using anisotropic and isotropic models for ordered and disordered films, respectively. The complex optical function spectra of gold[65] and ordered TCH_3[27,66] were taken from reported data, and those of ordered ODS were evaluated from independent measurements on polycrystalline samples of hydrolyzed OTS.[50,67] As discussed above (section 3.3.1), the residual ODS spectra for intermediate f_{OH} films appear best understood in terms of an island model with coexisting domains of conformationally ordered and disordered phases. Since there appears to be no straightforward way to obtain reliable reference optical functions for intermediately disordered alkyl chains, the simulations of intermediately ordered ODS overlayer films were carried out by approximating the structures as a composite of an oriented all-*trans* phase and a randomly oriented liquid phase. The optical function spectra of the latter were evaluated from independent measurements on liquid-phase OTS.[50]

Figure 9A shows a best fit ODS residual spectrum for the case a f_{OH} = 1.0 substrate. The simulation was made using the pure ordered-phase optical functions, and the fitting procedure involved adjusting the molecular tilt and chain twist until the best fit of the d^+ and d^- mode peaks to the experimental spectrum, also shown in Figure 9A, was reached. With this criterion, the best fit spectrum corresponds to an average chain in the assembly tilted by 10(±2)° from the surface normal with the C−C−C backbone twisted by 46(±2)° around the chain axis. However, discrepancies can be noted. In particular, the line widths appear slightly broader in the experimental spectrum and the CH_3 modes do not match quantitatively. The fit can be somewhat improved by the introduction of a small fraction (~5−10%) of a disordered ODS component, which suggests that the f_{OH} = 1.0 film might be slightly heterogeneous. However, we caution that small discrepancies in such fits are not well-understood, particularly for the CH_3 groups.[27,66]

For the $f_{OH} \lesssim 0.8$ films, reasonable fits only could be obtained with simulations based on heterogeneous ODS films having a sizeable fraction of disordered phase. While the quality of the fits was not sufficient to merit quantitative extraction of the composition, the results clearly indicate that these ODS overlayers consist of coexisting conformationally ordered and disordered phases. The general trend shows the liquid-like fraction to reach a *maximum* of 80−95% near $f_{OH} \sim 0.5$. Figure 9B shows the match between the f_{OH} = 0.5 experimental spectrum and a simulation for a 90:10 liquid/ordered ratio with the ordered chains oriented at 10°.

4. Discussion

4.1. Structures of Films Formed on Highly Hydrophilic ($f_{OH} \gtrsim 0.8-0.9$) Surfaces. All the experimental evidence indicates that the ODS films which form on very high f_{OH} surfaces consist of close-packed, nearly vertically oriented chains and exhibit extremely high oleophobic and hydrophobic wetting characters. These films exhibit nearly identical characteristics to those formed on SiO_2 surfaces under identical preparation conditions.[12,13,15]

The ODS film thicknesses calculated from the ellipsometric data reach a maximum value for $f_{OH} \gtrsim 0.8-0.9$. On the basis of a complete coverage reference state of vertically oriented chains packed at the density of polyethylene crystals, these thicknesses are equivalent to a monolayer coverage of 94(±3)%. This value agrees, within experimental errors, with those determined for dense-packed ODS monolayers prepared on the hydrated surfaces of oxidized silicon.[13b,32,34] The high contact angle values observed for water and hexadecane (θ_w = 114° and θ_{HD} = 46°) demonstrate that the monolayer surfaces consist of nearly perfect CH_3 group wetting character. The infrared spectra yield a number of important structural characteristics. The low peak frequency values (2849.4 and 2916.8 cm^{-1}, respectively) and narrow line widths of the d^+ and d^- modes are consistent with rodlike chains packed in a crystalline-like environment, while the strong chain wagging mode progressions in the low-frequency spectra demonstrate high-*trans* conformational ordering with ~6% average *gauche* content obtained from the interband spacings. The presence of a single, narrow CH_2 scissors deformation peak at 1467.5 cm^{-1} is indicative that the ODS chains are packed in a triclinic or hexagonal type of arrangement. Finally, spectral simulation of the d^+ and d^- mode intensities yields an average chain tilt of 10(±2)° from the surface normal with a 46(±2)° twist of the C−C−C plane around the chain axis. In support of the highly organized character of the alkyl chains, the low-frequency SiOSi and SiOH mode spectra suggest that the structural order in the underlying siloxy network is greatest with the high-f_{OH} substrates. Further, the analysis of the line shapes of the SiOSi stretching mode peak suggests that the siloxy network is composed of cyclic oligomers.

One apparent discrepancy in the above analysis is that, compared to a densest packed, vertically oriented monolayer of ODS chains, the ellipsometric coverage indicates a 6(±3)% lower surface density, whereas the 10(±2)° average chain tilt angle (from IRS) corresponds only to a 1.5% ((1 − cos 10°) × 100) lower surface density. However, these data can be reconciled with a heterogeneous monolayer structure of islands of ordered chains, most likely separated by line defects of missing chains between the islands. This structure is supported by the indication that the best fits between simulated and experimental infrared spectra for f_{OH} = 1.0 films contain a small fraction of disordered chains since the latter can be expected to arise at the edge of ordered domains. These types of molecular scale defects recently have been proposed for ODS monolayers on oxidized silicon.[13b] Recent atomic force microscope images

of ODS monolayers on oxidized silicon substrates reported by Silberzan and co-workers[68a] reveal ~200−300 nm polygon-shaped domains separated by ~2−8 Å wide lines between the domain edges. Schwartz et al.[68b] also report images of ODS monolayers on surfaces of hydroxylated mica, which indicate a presence of densely packed domains separated by domain edges (edge dimensions not reported).

4.2. Films Formed on Intermediately Hydrophilic Surfaces ($0 < f_{OH} \lesssim 0.8$). Over the range of intermediate wettability alkanethiolate surfaces ($0 < f_{OH} \lesssim 0.8$), the ODS films show continuously varying characteristics with changes in f_{OH}. While the coverages smoothly increase with increasing f_{OH}, the degree of chain disorder reaches a maximum in the midrange vicinity of $f_{OH} \sim 0.5$ surfaces.

The ellipsometric data show that between $f_{OH} = 0$ and ~0.8 the ODS coverage increases in an approximate linear fashion with increasing values of f_{OH}. Analysis of the contact angle data with eq 2 reveals that the CH_2 group reaches a maximum effective surface exposure of ~40% for the $f_{OH} \sim 0.5$ ODS film, a situation which requires significant folding and conformational disorder of the ODS chains.

The infrared spectra support the above conclusion and reveal further details that the structures are heterogeneous. At $f_{OH} \sim 0.5$ the residual ODS component spectra require the presence of extensively conformationally *disordered* ODS chains as shown by (1) maximum d^+ and d^- mode peak frequency values, (2) a minimally resolved contribution from the wag−twist progression, and (3) maxima in the d^+ and d^- band integrated intensities. On the other hand, the simultaneous presence of highly conformationally *ordered* ODS chains, regardless of the f_{OH} value is indicated by (1) the asymmetric d^+ and d^- mode line shapes, which can be fit by combinations of crystalline- and liquid-phase components, (2) the r^- mode line shapes, which for films outside of the $f_{OH} \sim 0.5$ region show the presence of ordered, vertically oriented chains, (3) vestiges of the wag−twist progression bands at all f_{OH} values, even in the $f_{OH} = 0.5$ film, and (4) a narrow CH_2 scissors deformation peak at all f_{OH} values. In concert with the above changes in the alkyl chain spectra, the siloxy network mode spectra change continuously with f_{OH} and the intensity of the SiOSi stretching mode peak shows a maximum in the vicinity of $f_{OH} \sim 0.5$. Although it is difficult to make a clear structural interpretation of the siloxy mode spectra, it does appear that the underlying siloxy network in the ODS films constantly restructures in terms of bond orientations and degree of cross-linking over the intermediate range of f_{OH} values.

All of the above evidence points to the existence of a series of structures which continuously vary with f_{OH} in terms of coexisting fractions of ordered and disordered ODS chains, with the maximum contribution of the disordered chains at $f_{OH} \sim 0.5$. Since it is difficult to conceive of any reasonable structure in which the ordered and disordered components exist in a uniform random mixture, *the most likely structure involves the coexistence of islands of close-packed all-trans molecules, oriented near vertical to the substrate surface, interpersed in a background of disordered molecules.*

4.3. The Substrate-Decoupling Mechanism of ODS Film Formation. All the results in this study can be understood within the framework of the recently proposed substrate-decoupling mechanism,[13] which predicts that densely packed, highly organized alkylsiloxane films form only when a uniform layer of water, in the range of one to several monolayers, is tenaciously bound to the substrate. Film formation proceeds by adsorption of solute species to form a freely mobile layer of hydrolyzed *n*-alkyltrichlorosilane molecules supported upon the water film, essentially the analog of a Langmuir film[69] with its associated structural phases. Below a specific temperature for each chain length[13] (T_c) densely packed liquid-condensed (LC) surfactant phases result at maximum adsorption. We note that T_c for C_{18} chains is 28(±5)°,[13b] a value higher than used in our film preparations. In the final stages of film formation, in-plane, intermolecular cross-linking of the molecular silanol groups occurs in a manner compliant with the established chain order.

4.3.1. $f_{OH} \gtrsim 0.9$ and $f_{OH} = 0$ Surfaces. This mechanism predicts that for fully wet substrate surface areas the overlayer films self-assemble to form structures determined only by adsorbate chain intermolecular interactions. Thus the film structures should be uncorrelated (incommensurate) with the actual substrate structure. In contrast, on water-free substrate surface regions no mechanism is available to allow surface hydrolysis of chlorosilane species and dynamic equilibration of Langmuir-type phases; accordingly, overlayer film formation must occur via random adsorption of solute alkylsilane species, some of which may already be partially cross-linked or aggregated, and by random, irreversible chemisorption at unhydrated alkanethiolate OH terminal groups. Thus, in the absence of substrate water films it is expected that any adsorbed alkylsiloxane films will be disordered.

The observed characteristics of the ODS films on the highly water wettable substrates, i.e. with $f_{OH} \gtrsim 0.9$, fit the above predictions. It is observed that the ODS forms a well-organized assembly of extended, oriented alkyl chains and that the packing arrangement is uncorrelated with that of the highly organized hydroxy-terminated alkanethiolate underlayer chains. In particular, the average molecular orientation of the chains in the ODS overlayer is 8−12°, while that of the underlying alkanethiolate monolayer is 26−30°.[3,66] In terms of translationally ordered arrangements of chains with hexagonal packing symmetry, the two layers represent different tilt phases, distinguished by different lattice spacings of the adsorbate pinning sites. Specifically, while the *average* spacing of the thiolate S atoms at maximum coverage on Au(111) is known to be 5.1 Å,[3,10] that of the chain pinning sites in an ideal 10° tilt phase would be 4.57 Å, on the basis of a 4.50 Å diameter alkyl chain. This comparison shows that the two lattices are quite incommensurate and thus clearly demonstrates that the organization of the chains in the ODS layer is driven by factors other than the geometry of the terminal alkanethiolate OH group superlattice. Further, the ODS structure appears nearly identical to that obtained on a hydrated SiO_2 surface,[13b] a substrate which exhibits ~5.0 nm^{-2} randomly distributed silanol (≡SiOH) groups,[70] in contrast to 4.6 nm^{-2} symmetrically distributed terminal OH groups on the alkanethiolate surface. In particular, a comparison of the ellipsometric coverages, water and hexadecane contact angles (advancing), d^+ and d^- peak frequencies, and average tilt angles shows the respective values for the $f_{OH} = 1$ and the SiO_2 substrates, respectively: 93(±3)%, 86−93%; 113(±2)°, 114-(±2)°; 46(±2)°, 45(±1)°; 2849.6(±0.3) cm^{-1}, 2848.8(±0.2) cm^{-1}; 2917.4(±0.5) cm^{-1}, 2916.8(±0.2) cm^{-1}; and 10(±2)°, 10(±2)°. This striking correspondence provides strong support for a substrate-independent formation mechanism on highly wettable surfaces. Additionally, we point out that chemical differences also seem unimportant since it is well-known that the chemical nature of these two types of OH groups is different; for example, ≡SiOH exhibits significantly stronger acidity than $-H_2COH$.

At the other extreme of wettability, the observed lack of affinity of the $f_{OH} = 0$ surface for ODS adsorption is understandable on the basis of the extremely high hydrophobicity of this surface. Further, since this surface is also extremely

oleophobic, the value of the equilibrium constant for adsorption of pre-cross-linked alkylsiloxane solute species from hexadecane solvent is expected to be orders of magnitude smaller relative to those for the higher energy $f_{OH} > 0$ surfaces, and thus the $f_{OH} = 0$ surfaces should remain adsorbate free, as observed.

4.3.2. $0 \lesssim f_{OH} \lesssim 0.8$ Surfaces. For alkanethiolate surfaces in the intermediate f_{OH} range, increasing f_{OH} leads to increasing water wettability (Figure 2) and continuously increasing ODS coverage (Figure 1) upon silanization. These observations reveal a simple correlation between hydrophilic character and ODS adsorption. More subtle is the pervasive observation of coexisting ordered and disordered ODS phases with a maximum disorder content near $f_{OH} \sim 0.5$. The Langmuir-like mechanism requires that the highly organized ODS component be formed on domains or patches of physisorbed water layers that are of multilayer thickness, in order to completely decouple the substrate, and that each span regions at least as large as the correlation lengths of the organized ODS domains (possibly ~5−10 nm; see section 4.3.1 above). As a corollary, disordered components then must be formed on isolated OH groups or highly localized water clusters. This picture provides a surface map (albeit somewhat crude) of substrate-bound water phases under the conditions of silanization. At low f_{OH}, where physisorbed water coverage is low, the appearance of a significant fraction of organized character in the (low-coverage) ODS films implies the existence of scattered patches of continuous water domains (at least $\gtrsim$ several nanometers) which can sustain some degree of organized self-assembly of adsorbed chains. With an increase of f_{OH} to ~0.5, the total water coverage is expected to increase, but the observed maximum in the ODS disordered fraction indicates that along with this increase there is a shift away from large patches toward small clusters. Finally, as f_{OH} increases well past ~0.5, the observed increase in the ODS chain organization implies the onset of domination of the surface by large water patches which grow to a continuous film in the $f_{OH} \sim 0.8-0.9$ region.

While no independent evidence appears available to *directly* test the above picture of the hydrated surfaces, several related pieces of information are available. First, UHV studies of D_2O adsorption on controlled composition OH/CH_3 mixed substrates,[71] identical to those used in the present study, show that above ~140 K the D_2O structure on $f_{OH} \gtrsim 0.8$ surfaces consists of a continuous film of water, while on the intermediate to low f_{OH} surfaces, clusters of variable sizes are formed. Second, based on perfectly *random* OH/CH_3 distributions, the onset of continuous water films, presumably bilayers or thicker, is theoretically predicted to occur above $f_{OH} \sim 0.5$ and $0.30 \lesssim f_{OH} \lesssim 0.45$ on the basis of simple percolation theory[72] and mean-field, lattice−gas model calculations, respectively.[17] Both of these models then predict that, under ideal conditions of maximum water adsorption, ODS adsorption should attain maximum coverages and highest organization starting at these low f_{OH} values, markedly contrary to the threshold of ~0.8 observed both in ODS absorption (Figure 2) and the D_2O cluster-wetting transition, mentioned above. Explanations for this sharp discrepancy are beyond the scope of the present study, but one factor to be considered is that the OH/CH_3 groups are clustered, rather than randomly distributed, as assumed in the theoretical models, with the degree of clustering dependent upon the value of f_{OH}. The latter possibility is supported by recent scanning tunneling microscopy observations of phase segregation in alkanethiolate monolayers of rather similar component C_{16} thiols[73] (CH_3/CO_2CH_3 terminated) as well as recent infrared spectroscopic, wetting, and secondary ion mass spectrometry studies[51,74] which indicate phase segregation in $C_{16}OH$-/CH_3-terminated mixed alkanethiolate monolayers. Until such complexities are experimentally characterized, further comparisons of adsorption and wetting phenomena with simple theoretical models do not appear fruitful.

4.4. Comparisons with Other Partially Disordered Alkyl Chain Monolayers. The ODS films for the high-f_{OH} surfaces appear to be satisfactorily described in terms of an approach to a structural limit of high surface coverage with long-range correlations. However, as the film coverages decrease, the structures become quite *heterogeneous*, with disorder maximized at coverages near 50% (near $f_{OH} \sim 0.5$ in Figure 1). The structures of these latter films can be contrasted quite usefully with a previously studied[5] ~50% coverage monolayer film of C_{18} *n*-alkoxide chains, covalently bonded to randomly distributed siloxy groups on amorphous SiO_2 surfaces, which exhibits *homogeneous* disorder, *viz.*, essentially molecularly uniform, random distributions of chains on the substrate. The structure of this C_{18} alkoxy film has been characterized as consisting of extended chain structures with relatively low *gauche* contents in which groups of neighboring chains cluster into "tufts" (presumably to maximize attractive interactions). The approximate values of the hexadecane and water contact angles (advancing), the d^- mode peak frequencies (residual spectra, Figure 6), and the calculated percent exposure of the CH_3 groups (from wetting data via eq 2) for the ODS and alkoxy/SiO_2 films, respectively, are[5,13b] 29(±2)° and 32(±3)°; 70° and 102(±3)°; 2925−2926 and 2921−2922.5 cm^{-1}; ~40 and 65−70%. Thus, in spite of the *identical chain lengths and quite similar overall surface coverages*, it is clear that the two films have *very different* structures. In particular, the differences in CH_3 group exposure and d^- frequencies indicate more severe chain folding in the $f_{OH} \sim 0.5$ ODS films than in the C_{18} alkoxy film. However, since the IRS data show evidence for a component (~5−20%) of conformationally ordered chains in the $f_{OH} \sim 0.5$ ODS films (Figure 6), the above observations of ODS film behavior are weighted by this ordered contribution, so it follows that the corresponding disordered component must be *significantly more disordered than the alkoxy/SiO_2 chains*, with the disorder approaching liquid-like chain structures, as also concluded from fits of simulated C−H stretching mode spectra (section 3.3.2). On this basis, the surface area occupied per ODS chain in the disordered regions of the $f_{OH} \sim 0.5$ films must be significantly greater than ~38 $Å^2$, the value for the 50% coverage alkoxy chains on the random SiO_2 lattice. Assigning values of ~50 $Å^2$ (corresponding to a very expanded LE Langmuir phase in which the corresponding average chain separation would be ~7 Å) and 19.5 $Å^2$ (95% (Figure 1) of 18.5 $Å^2$, the closest packed value of a 100% coverage film at 5.42 chains nm^{-2}; see section 3.1.2) to the ODS chain areas in the disordered and ordered regions, respectively, a simple mass balance shows that the observed (Figure 1) 50% coverage (corresponding to $2 \times 19.5 = 39$ $Å^2$/chain) for the $f_{OH} \sim 0.5$ films would consist of ~80% disordered and ~20% ordered chains, a distribution in good agreement with that of a 80−95% disordered component deduced from d^- band fitting (section 3.3.2). In terms of the Langmuir-like film formation mechanism, these results imply that near $f_{OH} \sim 0.5$, extended water domains occupy no more than 20% of the substrate surface, with the remaining minimum 80% occupied by unhydrated terminal OH groups or localized water clusters spaced on average $\gtrsim$7 Å apart. Again, we emphasize that this picture of the substrate surface applies to the sample under the ODS preparation conditions with a hexadecane/substrate interface.

Acknowledgment. The authors acknowledge valuable discussions with F. Rondelez. Financial support from the National

Science Foundation (DMR-900-1270, D.L.A., A.N.P., and S.V.A.), Dupont (M.H.), Procordia Science Foundation (B.L.), and the Swedish Research Council for Engineering Sciences (B.L.) is also acknowledged.

References and Notes

(1) Swalen, J. D.; Allara, D. L.; Andrade, J. D.; Chandross, E. A.; Garoff, S.; Israelachvilli, J.; McCarthy, T. J.; Murray, R.; Pease, R. F.; Rabolt, J. F.; Wayne, K. J.; Yu, H. *Langmuir* **1987**, *3*, 932−950.

(2) Ulman, A. *An Introduction to Ultrathin Organic Films, From Langmuir-Blodgett to Self-Assembly*; Academic Press: San Diego, CA, 1991.

(3) Dubois, L. H.; Nuzzo, R. G. *Annu. Rev. Phys. Chem.* **1992**, *43*, 437−463 and references cited therein.

(4) See, for examples: (a) Scheringer, M.; Hilfer, R.; Binder, K. *J. Chem. Phys.* **1992**, *96*, 2269−2277. (b) Kaganer, V. M.; Osipov, M. A.; Peterson, I. R. *J. Chem. Phys.* **1993**, *98*, 3512−527.

(5) Allara, D. L.; Parikh, A. N.; Judge, E. *J. Chem. Phys.* **1994**, *100*, 1761−1764.

(6) Collazo, N.; Rice, S. A. *Langmuir* **1991**, *7*, 3144−3153.

(7) (a) Di Meglio, J. M.; Shanahan, M. E. R. *C. R. Acad. Sci. Paris II* **1993**, *316*, 1543−1548. (b) Robbins, M. O.; Joanny, J. F. *Europhys. Lett.* **1987**, *3*, 729−735.

(8) (a) Joanny, J. F.; deGennes, P. G. *Physica (Amsterdam)* **1087**, *147A*, 238−255. (b) Redon, C.; Brochard-Wyart, F.; Rondelez, F. *Phys. Rev. Lett.* **1991**, *66*, 715−718. (c) Silberzan, P.; Leger, L. *Phys. Rev. Lett.* **1991**, *66*, 185−188.

(9) (a) Polymeropolous, E. E.; Sagiv, J. *J. Chem. Phys.* **1978**, *69*, 1836−1847. (b) Sabatini, E.; Rubeinstein, I.; Maoz, R.; Sagiv, J. *J. Electroanal. Chem.* **1987**, *219*, 365−371. (c) Kim, J.-H.; Cotton, T. M.; Uphaus, R. A. *J. Phys. Chem.* **1988**, *92*, 5572−5578. (d) Bard, A. J.; Abruna, H. D.; Chidsey, C. E.; Faulkner, L. R.; Feldberg, S. W.; Itaya, K.; Majda, M.; Melroy, M.; Murray, R. W.; Porter, M. D.; Soriaga, M. P.; White, H. S. *J. Phys. Chem.* **1993**, *97*, 7147−7174 and selected references cited therein.

(10) With regard to a superlattice structure, most evidence points to structures based on S atom distributions across a $(\sqrt{3} \times \sqrt{3})R30°$ unit mesh of the Au(111) substrate, the simplest pattern of which is just the $(\sqrt{3} \times \sqrt{3})R30°$ superlattice obtained from solution deposition; see, for example: (a) Strong, L.; Whitesides, G. M. *Langmuir* **1988**, *4*, 546−558. (b) Chidsey, C. E. D.; Loiacano, D. N. *Langmuir* **1990**, *6*, 682−691. (c) Chidsey, C. E. D.; Liu, G.-Y.; Rowntree, P. A.; Scoles, G. *J. Chem. Phys.* **1991**, *91*, 4421−4423. (d) Widrig, C. A.; Alves, C. A.; Porter, M. D. *J. Am. Chem. Soc.* **1991**, *113*, 2805−2810. (e) Dubois, L. H.; Zegarski, B. R.; Nuzzo, R. G. *J. Chem. Phys.* **1994**, *98*, 678−688.

(11) Recent X-ray diffraction evidence suggests that in well-annealed *n*-alkanethiolate SAMs prepared from solution the S atoms adopt a positional order commensurate with a $c(4\sqrt{3} \times 2\sqrt{3})$ structure with paired S atoms: Fenter, P.; Eberhardt, A.; Eisenberger, P. *Science* **1994**, *266*, 1216−1218.

(12) (a) Sagiv, J. *Isr. J. Chem.* **1979**, *78*, 339−345; 346−353. (b) Sagiv, J. *J. Am. Chem. Soc.* **1980**, *102*, 92−98. (c) Netzer, L.; Iscovici, R.; Sagiv, J. *Thin Solid Films* **1983**, *100*, 67−76. (d) Maoz, R.; Sagiv, J. *J. Colloid Interface Sci.* **1984**, *100*, 465−496. (e) Gun, J.; Iscovici, R.; Sagiv, J. *J. Colloid Interface Sci.* **1984**, *101*, 201−214. (f) Gun, J.; Sagiv, J. *J. Colloid Interface Sci.* **1986**, *112*, 457−472. (g) Tillman, N.; Ulman, A.; Schildkraut, J. S.; Penner, T. L. *J. Am. Chem. Soc.* **1988**, *111*, 6136−6144. (h) Wasserman, S. R.; Tao, Y.-T.; Whitesides, G. M. *Langmuir* **1989**, *5*, 1074−1087. (i) Silberzan, P.; Leger, L.; Aussere, D.; Benattar, J. J. *Langmuir* **1991**, *7*, 1647−1651. (j) Brzoska, J. B.; Shahidzadeh, N.; Rondelez, F. *Nature* **1992**, *360*, 719−721.

(13) (a) Brzoska, J. B.; Ben Azouz, I.; Rondelez, F. *Langmuir* **1994**, *10*, 4367−4373. (b) Parikh, A. N.; Allara, D. L.; Ben Azouz, I.; Rondelez, F. *J. Phys. Chem.* **1994**, *98*, 7577−7590.

(14) Finklea, H. O.; Robinson, L. R.; Blackburn, A.; Richter, B.; Allara, D.; Bright, T. *Langmuir* **1986**, *2*, 239−244.

(15) Allara, D. L.; Parikh, A. N.; Rondelez, F. accepted for publication in *Langmuir*.

(16) Ulman, A. *Adv. Mater.* **1990**, *2*, 573−582 and selected references cited therein.

(17) (a) Ulman, A.; Evans, S. D.; Shnidman, Y.; Sharma, R.; Eilers, J. E.; Chang, J. C. *J. Am. Chem. Soc.* **1991**, *113*, 1499−1506. (b) Ulman, A.; Evans, S. D.; Shnidman, Y.; Sharma, R.; Eilers, J. E. *Adv. Colloid Interface Sci.* **1992**, *39*, 175−224.

(18) Sanasay, P.; Evans, S. D. *Langmuir* **1993**, *9*, 1024−1027.

(19) (a) Netzer, L.; Sagiv, J. *J. Am. Chem. Soc.* **1983**, *105*, 674−676. (b) Netzer, L.; Iscovici, R.; Sagiv, J. *Thin Solid Films* **1983**, *105*, 674. (c) Pomerantz, M.; Segmuller, A.; Netzer, L.; Sagiv, J. *Thin Solid Films* **1985**, *132*, 153−162. (d) Tillman, N.; Ulman, A.; Penner, T. L. *Langmuir* **1989**, *5*, 101−111. (e) Ulman, A.; Tillman, N. *Langmuir* **1989**, *5*, 1418−1420.

(20) Nuzzo, R. G.; Fusco, F. A.; Allara, D. L. *J. Am. Chem. Soc.* **1987**, *109*, 2358−2367.

(21) Troughton, E. B.; Bain, C. D.; Whitesides, G. M.; Nuzzo, R. G.; Allara, D. L.; Porter, M. D. *Langmuir* **1988**, *4*, 365−385.

(22) Evans, S. D.; Sharma, R.; Ulman, A. *Langmuir* **1991**, *7*, 156−161.

(23) Tripp, C. P.; Hair, M. L. *Langmuir* **1992**, *8*, 1120−1126.

(24) (a) Bain, C. D.; Whitesides, G. M. *J. Am. Chem. Soc.* **1988**, *110*, 6560−6561. (b) Bain, C. D.; Evall, J.; Whitesides, G. M. *J. Am. Chem. Soc.* **1989**, *111*, 7155−7164.

(25) See, for example: Azzam, R. M. A.; Bashara, N. M. *Ellipsometry and Polarized Light*; North-Holland: Amsterdam, The Netherlands, 1977.

(26) The calculations reported here assume no change in the adsorbed water layer thickness upon ODS adsorption. However, it has been shown that there may be a fractional monolayer increase in the adsorbed water upon ODS film formation (Angst, D. L.; Simons, G. W. *Langmuir* **1991**, *7*, 2236−2242), and therefore accurate calculations should take this effect into account. Considering that a monolayer of water is only ~2−2.5 Å thick, the error is estimated to be within our experimental uncertainties.

(27) Parikh, A. N.; Allara, D. L. *J. Chem. Phys.* **1992**, *96*, 927−945.

(28) den Engelsen, D. *Surf. Sci.* **1976**, *56*, 272−280.

(29) (a) Maxwell-Garnett, J. C. *Phil. Trans.* **1904**, *203*, 385. (b) Maxwell-Garnett, J. C. *Phil. Trans.* **1906**, *205*, 237.

(30) Buontempo, J. T.; Rice, S. A. *J. Chem. Phys.* **1993**, *98*, 5835−5846.

(31) Nuzzo, R. G.; Dubois, L. H.; Allara, D. L. *J. Am. Chem. Soc.* **1990**, *112*, 558−569.

(32) Wasserman, S. R.; Whitesides, G. M.; Tidswell, I. M.; Ocko, B. M.; Pershan, P. S.; Axe, J. D. *J. Am. Chem. Soc.* **1989**, *111*, 5852−5861.

(33) Geil, P. H. *Polymer Single Crystals*; Wiley-Interscience: New York, NY, 1963.

(34) Tidswell, I. M.; Rabedeau, T. A.; Pershan, P. S.; Kosowsky, S. D.; Folkers, J. P.; Whitesides, G. M. *J. Chem. Phys.* **1991**, *95*, 2854−2861.

(35) In a few cases, it was noted that ODS films of <5% coverages appeared to form. It was concluded that these cases arose when the initial RS films were formed on unusually rough substrates formed during poorly controlled Au depositions. It would appear from the IRS and wetting data that the ODS chains actually are incorporated into void defects in the RS films.

(36) (a) Bain, C. D.; Troughton, E. B.; Tao, Y.-T.; Evall, J.; Whitesides, G. M.; Nuzzo, R. G. *J. Am. Chem. Soc.* **1989**, *111*, 321−335. (b) Fox, H. W.; Zisman, W. A. *J. Colloid Sci.* **1952**, *7*, 428−442.

(37) Michel, B.; Rohrer, H.; Häussling, L.; Ringsdorf, H. *Angew. Chem., Int. Ed. Engl.* **1990**, *30*, 569−572.

(38) Hautman, J.; Klein, M. L. *Phys. Rev. Lett.* **1991**, *67*, 1763−1766.

(39) Holmes-Farley, S. R.; Bain, C. D.; Whitesides, G. M. *Langmuir* **1988**, *4*, 921−937.

(40) See for example: Israelachvilli, J. *Intermolecular and Surface Forces: With Application to Colloidal and Biological Systems*; Academic Press: London, 1985.

(41) Cassie, A. B. D. *Discuss. Faraday Soc.* **1948**, *3*, 11−16.

(42) (a) Neumann, A. W.; Good, R. J. *J. Colloid Interface Sci.* **1975**, *38*, 341−350. (b) Schwartz, L. W.; Garoff, S. *Langmuir* **1985**, *1*, 219−230. (c) Joanny, J. F.; de Gennes, P.-G. *J. Chem. Phys.* **1984**, *81*, 552−562.

(43) Bertilsson, L.; Liedberg, B. *Langmuir* **1993**, *9*, 141−149.

(44) Atre, S. V.; Liedberg, B.; Allara, D. L. Submitted for publication.

(45) A recent study has shown that for unequal chain length OH- and CH_3-terminated thiol monolayers the r^- intensity does not provide a reliable estimate of the film composition (ref 44).

(46) (a) Snyder, R. G. *Spectrochim. Acta* **1963**, *19*, 85−116. (b) MacPhail, R. A.; Strauss, H. L.; Snyder, R. G.; Elliger, C. A. *J. Phys. Chem.* **1982**, *88*, 334−341. (c) Snyder, R. G.; Hsu, S. L.; Krimm, S. *Spectrochim. Acta Part A* **1978**, *34*, 395−406. (d) Hill, I. R.; Lewin, I. W. *J. Chem. Phys.* **1979**, *70*, 842−581.

(47) Snyder, R. G.; Strauss, H. L.; Elliger, C. A. *J. Phys. Chem.* **1982**, *86*, 5145−5150.

(48) (a) Wood, K. A.; Snyder, R. G.; Strauss, H. L. *J. Chem. Phys.* **1989**, *91*, 5255−5267. (b) Cameron, D. J.; Casal, H. L.; Mantsch, H. H. *Biochemistry* **1980**, *19*, 3665−3672.

(49) In principle, quantitative analyses of the integrated intensities of the two component peaks could be used to obtain accurate values of the actual *trans/gauche* contents. However, these analyses were not attempted because of the complicating factors of chain orientation, overlap of Fermi resonance features with the d^- mode peak, and changes in the intrinsic oscillator strength with the conformational order.

(50) Parikh, A. N.; Schivley, M. A.; Allara, D. L. Manuscript in preparation.

(51) Atre, S. V.; Liedberg, B.; Allara, D. L. Manuscript in preparation.

(52) Allara, D. L.; Nuzzo, R. G. *Langmuir* **1985**, *1*, 52−64.

(53) Adrianoc, K. A.; Izmaylov, B. A. *J. Organomet. Chem.* **1967**, *8*, 435−441.

(54) Lipp, E. D.; Smith, A. L. *The Analytical Chemistry of Silicones*; Smith, A. L., Ed.; Wiley: New York, 1991; pp 305−345, and selected references cited therein.

(55) Bellamy, L. J. *Infrared Spectra of Complex Molecules*, ed. 3; Chapman and Hall: London, 1975; Vol. 1, pp 374−383.

(56) Some combination of three possible factors for each mode will control these changes: (1) variation of the magnitude of the transition dipole moment, (2) reorientation of the molecular groups with respect to the surface, and (3) changes in the total number of the associated molecular unit, *viz.*, SiOSi and SiOH, per unit area of surface. The latter is a function both of the total ODS coverage and the degree of cross-linking of the siloxy network since each cross-link event condenses a pair of SiOH units into one SiOSi unit. At present, it does not appear possible to untangle the above factors in any quantitative way for three reasons: (1) two possibilities exist for the mode assignmentt of the lower frequency band, (2) the optical function spectrum has not been measured for the SiOSi stretching mode, and (3) an accurate description is not available for the specific atom trajectories and charge flow direction (transition dipole) in the latter mode.

(57) See, for example: (a) Boyd, I. W.; Wilson, J. B. *Appl. Phys. Lett.* **1987**, *50*, 320−322. (b) Boyd, I. W. *Appl. Phys. Lett.* **1987**, *51*, 418−420.

(58) (a) Jones, R. N.; McKay, A. F.; Sinclair, R. G. *Phil. Trans. R. Soc. Chem.* **1952**, *A74*, 2575−2578. (b) Brown, J. K.; Sheppard, N.; Simpson, D. M. *Phil. Trans. R. Soc. Chem.* **1957**, *A247*, 35. (c) Snyder, R. G. *J. Mol. Spectrosc.* **1960**, *4*, 411−434. (d) Snyder, R. G. *J. Chem. Phys.* **1967**, *47*, 1316−1358.

(59) In analyzing the spectra in Figure 9, both the ODS and the *n*-alkanethiolate chains must be considered as potential sources of the observed peak series, but two pieces of evidence definitively support assignment to the ODS alkyl chains. First, both the present and published spectra of highly *trans n*-alkanethiolate assemblies[31] on gold, taken under identical spectral conditions, show much weaker features in this frequency region than observed for the ODS/RS composite film spectra, and it is not expected that these intensities will increase simply because an ODS overlayer is present. The weak nature of these RS/Au monolayer wag−twist peaks is rationalized on the basis of the known effect of the terminal group in modulating the magnitude of the wag−twist transition dipole moment[58] with the conclusion that the thiolate end group leads to a relatively weak intensity compared to a variety of other groups. In particular, recent studies of hydrolyzed bulk OTS molecules reveal wag−twist intensities which are significantly higher on a per molecule basis than those of the corresponding polycrystalline octadecane thiol or disulfide compounds.[50] Second, these same wag−twist features also have been observed, with intensities comparable to the $f_{OH} = 1$ spectra in Figure 5, for spectra of ODS monolayers on hydrated gold surfaces,[14,15] a case for which no underlying thiolate layer is present to complicate the interpretation.

(60) Snyder, R. G.; Schachtschneider, J. H. *Spectrochim. Acta, Part A* **1963**, *19*, 85−116.

(61) Snyder, R. G.; Schachtschneider, J. H. *Spectrochim. Acta, Part A* **1963**, *19*, 117−168.

(62) Snyder, R. G. *Macromolecules* **1990**, *23*, 2081−2087.

(63) Snyder, R. G. *J. Mol. Spectrosc.* **1961**, *7*, 1161.

(64) Yeh, P. *Optical Waves in Layered Media*; Wiley-Interscience: New York, 1980.

(65) *Handbook of Optical Constants of Solids II*; Palik, E. D., Ed.; Academic: Orlando, FL, 1985.

(66) Laibinis, P. E.; Whitesides, G. M.; Allara, D. L.; Tao, Y.-T.; Parikh, A. N.; Nuzzo, R. G. *J. Am. Chem. Soc.* **1991**, *113*, 7152−7167.

(67) The optical tensor matrix element contributions of individual vibrational modes (oscillators) were determined from reference samples consisting of a set of several different monofunctional octadecyl compounds formed into KBr disks, bulk-liquid-phase samples of hydrolyzed OTS in a 45° prism cell, and KBr disks of polycrystallites of octadecylsiloxanes obtained by extensive deliberate hydrolysis of OTS. Spectra of the solids were collected above and below the melting transitions, and consistent correlations between the relative changes in the mode intensities of the $d^{\pm}$ mode features with melting were established. These measurements were used to set the basis for the correct intensity of the desired optical functions and consistent intensity relationships between solid- and liquid-phase spectra for the reference compounds were used to correct for structural phase differences in the spectra. Complete details of these calculations will be presented elsewhere together with the optical function data.

(68) (a) Barrat, A.; Silberzan, P.; Bourdieu, L.; Chatenay, D. *Europhys. Lett.* **1992**, *20*, 633−638. (b) Schwartz, D. K.; Steinberg, S.; Israelachvilli, J.; Zasadzinski, J. A. N. *Phys. Rev. Lett.* **1992**, *69*, 3354−3357.

(69) Gaines, G. L., Jr. *Insoluble Monolayer at Liquid-Gas Interfaces*; Wiley-*Interscience*: New York, NY, 1966.

(70) (a) Kruger, A. A. *Surface and Near Surface Chemistry of Oxide Materials*; Novotny, J., Dufour, L. C., Eds.; Elsevier: Amsterdam, 1985; pp 413−448. (b) Zhuravlev, L. T. *Langmuir* **1987**, *3*, 316−318.

(71) Engquist, I.; Liedberg, B. and Engquist, I.; Liedberg, B.; Parikh, A.; Allara, D. Manuscripts in preparation. Indirectly relevant experimental data on the adsorption of H_2O vapor on functionalized surfaces at low temperatures also are available. Nuzzo et al. (Nuzzo, R. G.; Zegarski, B. R.; Korenic, E. M.; Dubois, L. H. *J. Phys. Chem.* **1992**, *96*, 1355−1361) have shown, using a combination of IRS and thermal programmed desorption measurements, that a condensed water layer heated above 140 K does not wet a pure CH_3 surface but rather organizes in the form of clusters, but, in contrast, a hydrophilic surface of pure CO_2H groups yields continuous water films.

(72) Stauffer, D. *Introduction to Percolation Theory*; Taylor and Francis: London, 1985.

(73) Stranick, S.; Parikh, A. N.; Tao, Y.-T.; Allara, D. L.; Weiss, P. S. *J. Phys. Chem.* **1994**, *98*, 7636−7646.

(74) Wood, M.; Atre, S. V.; Liedberg, B.; Zhou, Y.; Allara, D. L.; Winograd, N. Manuscript in preparation.

JP9503728